mathematics

MDPI

Article

The Effects of Variable Thermal Conductivity in Thermoelastic Interactions in an Infinite Material with and without Kirchhoff's Transformation

Aatef Hobiny [1] and Ibrahim Abbas [1,2,*]

[1] Mathematics Department, Faculty of Science, King Abdulaziz University, Jeddah 22254, Saudi Arabia
[2] Mathematics Department, Faculty of Science, Sohag University, Sohag 82524, Egypt
* Correspondence: ibrabbas7@science.sohag.edu.eg

Abstract: In this paper, the problem of an unbonded material under variable thermal conductivity with and without Kirchhoff's transformations is investigated. The context of the problem is the generalized thermoelasticity model. The boundary plane of the medium is exposed to a thermal shock that is time-dependent and considered to be traction-free. Because nonlinear formulations are difficult, the finite element method is applied to solve the problem without Kirchhoff's transformations. In a linear case, when using Kirchhoff's transformations, the problem's solution is derived using the Laplace transforms and the eigenvalue approach. The effect of variable thermal conductivity is discussed and compared with and without Kirchhoff's transformations. The graphical representations of numerical results are shown for the distributions of temperature, displacement and stress.

Keywords: finite element method; eigenvalue approach; Laplace transform variable thermal conductivity; Kirchhoff's transform

MSC: 74H15

Citation: Hobiny, A.; Abbas, I. The Effects of Variable Thermal Conductivity in Thermoelastic Interactions in an Infinite Material with and without Kirchhoff's Transformation. *Mathematics* **2022**, *10*, 4176. https://doi.org/10.3390/math10224176

Academic Editors: Vicente Martínez and Pablo Gregori

Received: 21 September 2022
Accepted: 4 November 2022
Published: 8 November 2022

1. Introduction

Previously, it had been considered that all thermal parameters in thermoelasticity theory were independent of temperature. However, considering many materials' theoretical and actual findings at high temperatures Noda [1] published a thorough analysis of temperature-dependent material characteristics in 1991 and demonstrated that the materials' thermal conductivity drops off exponentially as the temperature rises. The importance of thermoelastic materials with variable heat conductivity is a result of their recent employment in a variety of intriguing applications, primarily in contemporary technology regarding new energy sources. In applied mechanical sciences and steel stress analysis, which is the most typically designed structural material, the thermoelastic theory is crucial.

It may represent the solid mechanical properties of various common elastic materials, including coal, concrete and wood. However, it is unable to capture the mechanical behavior of several synthetic polymer and clastomer kinds, including polyethylene. The thermoelastic theory has recently received greater attention due to its practical applications in a variety of domains, including engineering, constructions, geology, biology, geophysics, acoustics, physics, plasma, etc.

The theory formulated by Lord and Shulman [2] calculates the motion caused by a thermal field's limited speed, using only one relaxation time. For an unbounded medium with spherical cavities, Youssef et al. [3] studied the dependence of the material's thermal conductivity and elastic modulus on temperature. Sherief and Hamza [4] presented the modeling of varying thermal conductivity in an infinitely thermoelastic hollow cylinder. In 2D thermoelasticity problems with a temperature-dependent elastic modulus, Othman [5] investigated the thermoelastic interactions. In their analysis of a problem

involving density and thermoelastic properties that vary with temperature, Zenkour and Abbas [6] identified several defining characteristics of temperature-dependent properties of the material. Abbas [7] applied the finite element approaches to investigate the generalized magneto-thermoelastic interaction in nonhomogeneous isotropic cylinders. Abouregal and Sedighi [8] used the Moore–Gibson–Thompson heating conduction model to study the effects of rotation and varying properties in visco-thermo-elastic orthotropic cylinders. Xiong and Guo [9] studied the effects of varying properties and moving heating sources on magneto-thermoelasticity problems with fractional-order thermoelastic models.

Thermal conductivity is an essential material property that is often assumed to be constant. Several theoretical and experimental studies, however, have shown that thermal conductivity is strongly connected to the temperature change [10–19]. Othman et al. [20] discussed the effect of initial stress and variable thermal conductivity on an unbounded fiber-reinforced thick plate. Xiong et al. [21] studied the effects of variable thermal conductivity on a thermoelasticity problem in an anisotropic fiber-reinforced plane. In a semiconducting medium with cylinder-shaped holes and varying thermal conductivity, Abbas et al. [22] investigated the solutions of photothermal interactions. Alzahrani [23] investigated the effects of varying thermal conductivity in semi-conducting materials. Convective fins with varying thermal conductivity and thermal generation were the subject of a thermal analysis study by Ghasemi et al. [24]. The impact of varying thermal conductivity on transients temperature fluctuations within wall-embedded insulation was studied by Khoukhi et al. [25]. Othman et al. [26] studied the effects of initial stress on semiconducting materials under temperature-dependent properties under the dual phase lag model. Several researchers [27–33] proposed solutions to various problems using extended thermoelastic theories.

This research aims to investigate the effects of thermal conductivity variations on the thermoelastic wave propagation of material. The finite element method was applied to solve the nonlinear problem (without Kirchhoff's transform). The Laplace transform and the eigenvalues approach was used to solve the linear problem (with Kirchhoff's transform). The numerical results for all physical quantities are obtained and visually displayed. A comparison is made between the numerical solutions and earlier analytical solutions produced by others while ignoring the new parameter, and the behaviors of the solution are investigated to validate the proposed method's correctness. The variable thermal conductivity is addressed and contrasted with and without Kirchhoff's transformations.

2. Basic Equations

The basic formulations of a homogeneous elastic material with variable thermal conductivity in the absence of body forces and thermal sources can be expressed as [2]:

The equations of motion

$$\mu u_{i,jj} + (\lambda + \mu) u_{j,ij} - \gamma T_{,i} = \rho \frac{\partial^2 u_i}{\partial t^2}. \tag{1}$$

The energy equation

$$\left(KT_{,j}\right)_j = \left(1 + \tau_o \frac{\partial}{\partial t}\right)\left(\rho c_e \frac{\partial T}{\partial t} + \gamma T_o \frac{\partial u_{j,j}}{\partial t}\right). \tag{2}$$

The constitutive equations

$$\sigma_{ij} = (\lambda u_{k,k} - \gamma T)\delta_{ij} + \mu\left(u_{i,j} + u_{j,i}\right), \tag{3}$$

Where T is the temperature, T_0 is the reference temperature, λ, μ are the Lame's constants, c_e is the specific heat at constant strain, $\gamma = (3\lambda + 2\mu)\alpha_t$, α_t is the coefficient of linear thermal expansion, ρ is the medium density, t is the time, e_{ij} are the components of the strain tensor, u_i are the components of the displacement vector, τ_o is the thermal relaxation time, δ_{ij} is the Kronecker symbol, the tensor is the components of stress tensor,

and K represents the temperature-dependent thermal conductivity and has the following linear form [34]

$$K(T) = K_o(1 + K_v T), \tag{4}$$

where K_o is the thermal conductivity when $T = T_o$, K_v is a parameter that is not positive. Let us take a look at an elastic material whose state may be described as functions of the spatial variables x and the time t, allowing the nonlinear Equation (1) to (3) to be provided by [34]:

$$(\lambda + 2\mu)\frac{\partial^2 u}{\partial x^2} - \gamma\frac{\partial T}{\partial x} = \rho\frac{\partial^2 u}{\partial t^2}, \tag{5}$$

$$K_o(1 + K_v T)\frac{\partial^2 T}{\partial x^2} + K_o K_v\left(\frac{\partial T}{\partial x}\right)^2 = \left(1 + \tau_o\frac{\partial}{\partial t}\right)\left(\rho c_e\frac{\partial T}{\partial t} + \gamma T_o\frac{\partial^2 u}{\partial t \partial x}\right), \tag{6}$$

$$\sigma_{xx} = (\lambda + 2\mu)\frac{\partial u}{\partial x} - \gamma T. \tag{7}$$

3. Application

The starting conditions are expected to be homogenous while the boundary condition at $x = 0$ may be taken into consideration,

$$u(0, t) = 0, T(0, t) = T_1 H(t), \tag{8}$$

where $H(t)$ is the Heaviside unit function and T_1 is a constant temperature. The non-dimensional parameters may now be written as

$$(x', u') = \eta c(x, u), K_v' = T_o K_v, T' = \frac{T}{T_o}, \sigma_{xx}' = \frac{\sigma_{xx}}{\lambda + 2\mu}, (t', \tau') = \eta c^2(t, \tau), \tag{9}$$

where $c^2 = \frac{\lambda+2\mu}{\rho}$ and $\eta = \frac{\rho c_e}{K}$.

The nonlinear governing equations with the dashes removed may be written as using non-dimensional form parameters (9)

$$\frac{\partial^2 u}{\partial x^2} - u_1\frac{\partial T}{\partial x} = \frac{\partial^2 u}{\partial t^2}, \tag{10}$$

$$(1 + K_v T)\frac{\partial^2 T}{\partial x^2} + K_v\left(\frac{\partial T}{\partial x}\right)^2 = \left(1 + \tau_o\frac{\partial}{\partial t}\right)\left(\frac{\partial T}{\partial t} + t_1\frac{\partial^2 u}{\partial t \partial x}\right), \tag{11}$$

$$\sigma_{xx} = \frac{\partial u}{\partial x} - u_1 T, \tag{12}$$

$$u(0, t) = 0,\ T(0, t) = T_1 H(t), \tag{13}$$

where $u_1 = \frac{\gamma T_o}{\lambda+2\mu}$, $t_1 = \frac{\gamma}{\rho c_e}$.

4. Numerical Scheme

The basic formulations established in this section are nonlinear partial differential equations. The finite element method (FEM) is being studied for solutions to this problem. The typical weak formulations processes, as described in [35], are applied in this approach. The fundamental formulations' non-dimensional weak formulations are fixed. The sets of independent weight function consisting of displacement δu and temperature δT are shown. The controlling formulations are multiplied by the independent weight function before integrating across the locative domain using the boundary conditions of problem. As a result, the nodal values for displacement and temperature may be stated as

$$T = \sum_{j=1}^{n} N_j T_j(t),\ u = \sum_{j=1}^{n} N_j u_j(t), \tag{14}$$

where n is the number of elements per node and N denotes the shape functions. Thus, as part of Galerkin's conventional procedures, the form and test functions are the same. Therefore,

$$\delta T = \sum_{j=1}^{n} N_j \delta T_j,\ \delta u = \sum_{j=1}^{n} N_j \delta u_j. \tag{15}$$

The three-node quadratic element is used. The one-dimension quadratic element is employed in this problem, and we assume that the master element, which may be specified by local coordinates in the range $[-1,\ 1]$, is used, which can be defined by

$$N_1 = \tfrac{1}{2}\chi(\chi - 1), \quad N_1 = 1 - \chi^2, \quad N_3 = \tfrac{1}{2}\chi(\chi + 1).$$

The following stage should include calculating the time derivative of the unknown variables using implicit methods. The weak formulas for FEM corresponding to (10-11) are now as follows.

$$\int_0^L \frac{\partial \delta u}{\partial x}\left(\frac{\partial u}{\partial x} - u_1 T\right)dx + \int_0^L \delta u\left(\frac{\partial^2 u}{\partial t^2}\right)dx = \delta u\left(\frac{\partial u}{\partial x} - u_1 T\right)_0^L, \tag{16}$$

$$\int_0^L \frac{\partial \delta T}{\partial x}\left((1 + K_v T)\frac{\partial T}{\partial x}\right)dx + \int_0^L \delta T\left(1 + \tau_o \frac{\partial}{\partial t}\right)\left(\frac{\partial T}{\partial t} + t_1 \frac{\partial^2 u}{\partial t \partial x}\right)dx = \delta T\left((1 + K_v T)\frac{\partial T}{\partial x}\right)_0^L, \tag{17}$$

where L is. the length of the domain.

5. Linear Case (with Kirchhoff's Transformation)

To transform the basic formulations into the linear form from the nonlinear one, we apply Kirchhoff's transform mapping [34] to variable thermal conductivity, which is presented in Equation (4)

$$\theta = \frac{1}{K_o}\int_0^T K(T)dT, \tag{18}$$

where the newly introduced function expresses heat conduction. We may obtain [34] by substituting from Equation (18) to (4), then integrating.

$$\theta = T + \frac{1}{2}K_v T^2. \tag{19}$$

From Equations (18) and (19), the following may be deduced:

$$K_o \theta_{,i} = K(T)T_{,i},\ K_o \theta_{,ii} = (K(T)T_{,i})_{,i},\ K_o \frac{\partial \theta}{\partial t} = K(T)\frac{\partial T}{\partial t}. \tag{20}$$

The governing Equation (10) through (13) may thus be expressed in the linear form:

$$\frac{\partial^2 u}{\partial x^2} - u_1 \frac{\partial \theta}{\partial x} = \frac{\partial^2 u}{\partial t^2}, \tag{21}$$

$$\frac{\partial^2 \theta}{\partial x^2} = \left(1 + \tau_o \frac{\partial}{\partial t}\right)\left(\frac{\partial \theta}{\partial t} + t_1 \frac{\partial^2 u}{\partial t \partial x}\right), \tag{22}$$

$$\sigma_{xx} = \frac{\partial u}{\partial x} - u_1 T, \tag{23}$$

$$T = \frac{1}{K_v}\left(-1 + \sqrt{1 + 2K_v \theta}\right), \tag{24}$$

$$u(0,t) = 0,\ \theta(0,t) = T_1 H(t) + \frac{1}{2}K_v (T_1 H(t))^2, \tag{25}$$

By applying Laplace transform to Equation (21) through (25),

$$\overline{f}(x,s) = L[f(x,t)] = \int_0^\infty f(x,t)e^{-st}dt. \tag{26}$$

Hence, we can get the following equations

$$\frac{d^2\overline{u}}{dx^2} = s^2\overline{u} + u_1\frac{d\overline{\theta}}{dx}, \tag{27}$$

$$\frac{d^2\overline{\theta}}{dx^2} = \left(s + s^2\tau_o\right)\left(\overline{\theta} + t_1\frac{d\overline{u}}{dx}\right), \tag{28}$$

$$\overline{u}(0,t) = 0, \overline{\theta}(0,s) = \frac{T_1}{s}\left(1 + \frac{1}{2s}T_1K_v\right). \tag{29}$$

From Equations (27) and (28), the vector-matrix differential equation can be expressed by

$$\frac{d\mathrm{V}}{dx} = AV, \tag{30}$$

where $V = \left(\overline{u} \quad \overline{\theta} \quad \frac{d\overline{u}}{dx} \quad \frac{d\overline{\theta}}{dx}\right)^T$ and $A = \begin{pmatrix} 0 & 0 & 1 & 0 \\ 0 & 0 & 0 & 1 \\ a_{31} & 0 & 0 & a_{34} \\ 0 & a_{42} & a_{43} & 0 \end{pmatrix}$ and $a_{31} = s^2$,

$$a_{34} = u_1,\ a_{42} = s + s^2\tau_o,\ a_{43} = \left(s + s^2\tau_o\right)t_1.$$

By using the eigenvalue technique as described in [36–43] regarding the solutions of Equation (30), the characteristic relation of matrix A may be expressed as

$$m^4 - (a_{31} + a_{42} + a_{34}a_{43})m^2 + a_{31}a_{42} = 0, \tag{31}$$

The matrix eigenvalues of A are the Equation (31); four roots which are defined by $\pm m_1$, $\pm m_2$. The solutions Equation (31) are given as

$$\mathrm{V}(x,s) = \sum_{i=1}^{2}\left(A_iX_ie^{-m_ix} + A_{i+1}X_{i+1}e^{m_ix}\right), \tag{32}$$

Where the boundary conditions of the problem can be used to compute the constants A_1, A_2, A_3, and A_4. The Stehfest technique [44] may be used as a numerical inversion strategy to obtain the temperature, displacement, and stress distribution final solutions.

6. Results and Discussion

In this study, the thermoelastic interaction resulting from a moving heat source under generalized thermoelastic models is investigated in an unbounded isotropic medium. The material specifications are specified below [45]:

$$\mu = 3.86 \times 10^{10}(kg)(m)^{-1}(s)^{-2}, K = 3.68 \times 10^2(kg)(m)\ (K)^{-1}(s)^{-3}, t = 0.6, T_1 = 1$$
$$T_0 = 293(K),\ \lambda = 7.76 \times 10^{10}(kg)(m)^{-1}(s)^{-2},\ c_e = 3.831 \times 10^2(m)^2(K)^{-1}(s)^{-2},$$
$$\alpha_t = 17.8 \times 10^{-6}(K)^{-1},\ \rho = 8.954 \times 10^3(kg)(m)^{-3}.$$

The numerical computations of physical quantities with regard to the distance x while taking variable thermal conductivity into account are performed within the framework of extended thermoelastic theory with and without Kirchhoff's transforms, as illustrated in Figures 1–12. Numerical calculations are carried out by the provided set of constants for the field distribution, displacement distribution (strain waves), temperature distribution (thermal waves) and mechanical waves distributions; numerical computations are per-

formed. During the time $t = 0.6$, the numerical computation was executed. The grid size was adjusted until the values of the fields under consideration settle. Further modification of mesh size above 20,000 elements does not significantly change the results. Thus, the grid size of 20,000 was used for this study. Figures 1–3 show the impacts of varying thermal conductivity in the temperature, the displacement, and the stress along the distance x without Kirchhoff transform (nonlinear case). Figure 1 depicts the temperature change as a function of distance x. It was seen to have a maximum value $(T_1 = 1)$ that satisfies the boundary conditions of the problem on the surface $x = 0$, after which the temperature decreases as x increases until it approaches zero. Figure 2 depicts the displacement variation as a function of distances x. It was discovered that the displacement achieves maximum negative values, gradually increasing until it reaches peak values near the surface, and then falls continuously to zero. Figure 3 shows the variations of stress as a function of distance x. The stress is shown to start at zero, which fulfills the problem boundary condition, and gradually rise up to positive peak values before decreasing heavily to negative peak values and increasing again to near zero. As predicted, varying thermal conductivity has a significant influence on the values of temperature, displacement, and stress distributions.

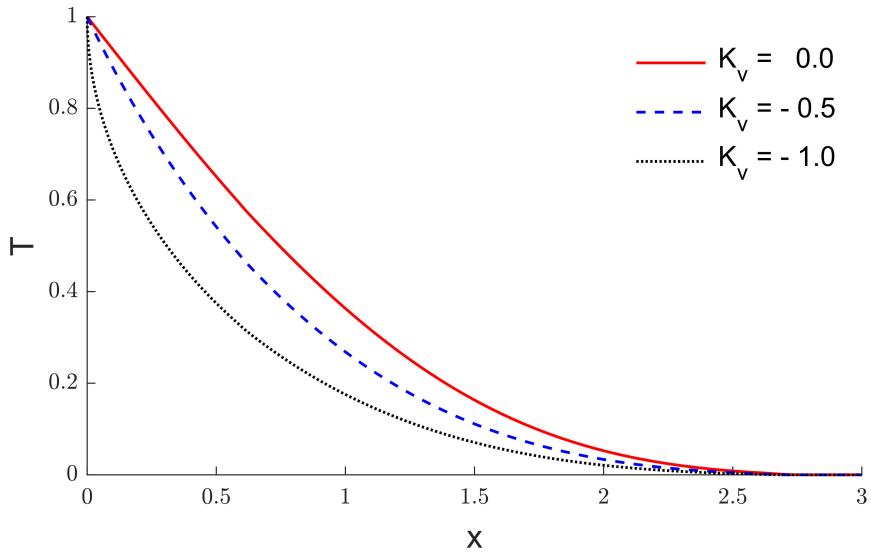

Figure 1. The temperature variation along the distance with three values of K_v.

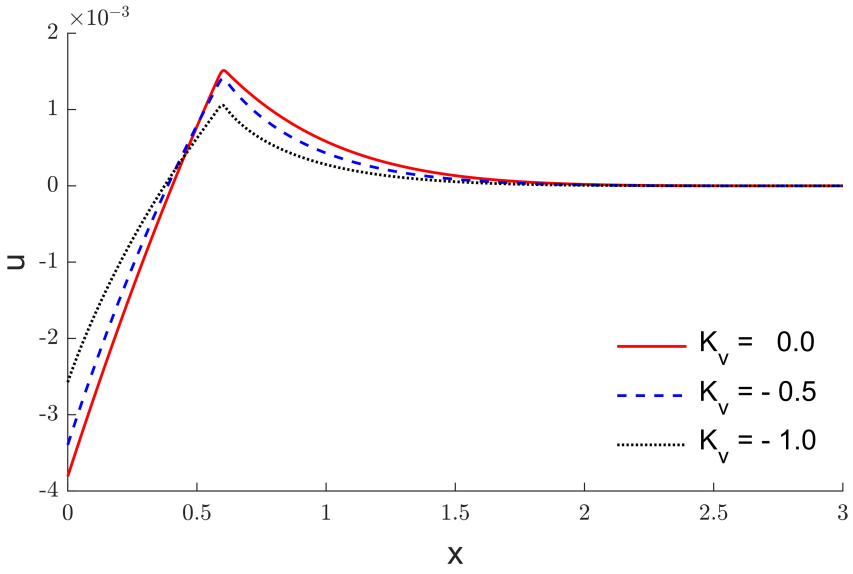

Figure 2. The variation of displacement with respect to the distances with three values of K_v.

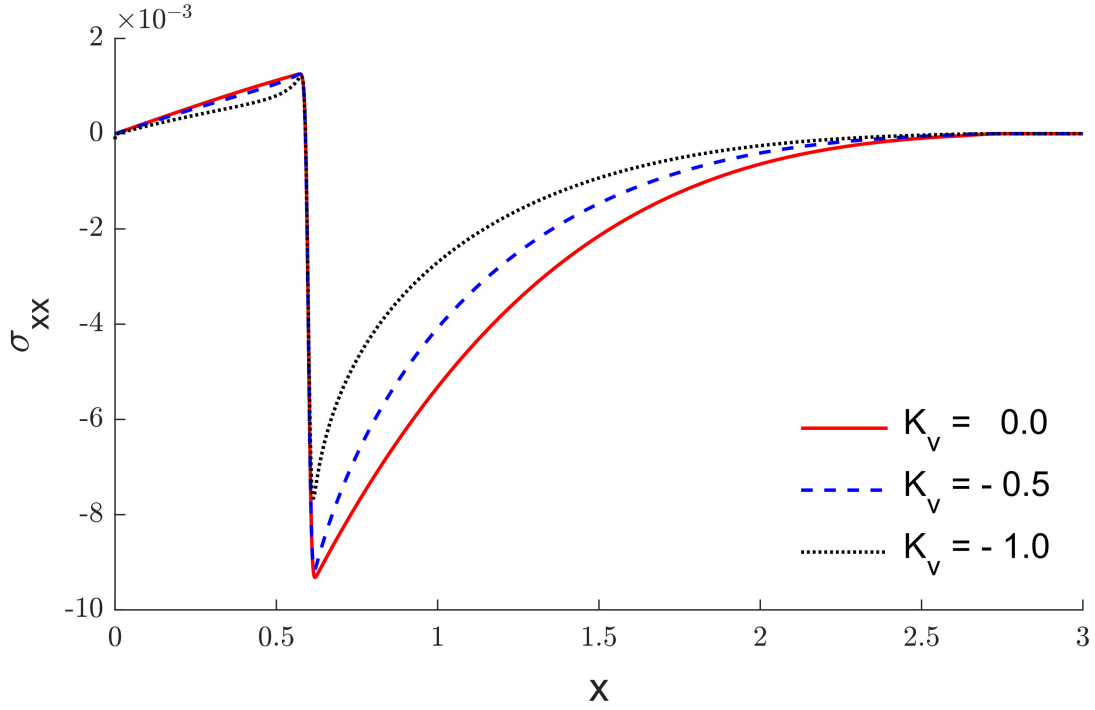

Figure 3. The stress variation via the distance with three values of K_v.

The difference between the use of Kirchhoff transform (WKT) and non-Kirchhoff transform (NKT) is seen in Figures 4–12. Figures 4–6 show the variations of temperature, the variations of displacement, and the variations of stress along the distance x when $k_v = -1$. It is observed that the solid line refers to the use of Kirchhoff transform (WKT) while the dotted line refers to the nonlinear case without Kirchhoff transform (NKT). The curves match at the surface according to the boundary condition of the temperature $(T_1 = 1)$ then the difference ratio increases with the increase of distance until $x = 0.75$ after that the difference ratio decreases to reach zero at $x = 2.55$ as in Figure 4. Figure 5 shows the displacement variations with Kirchhoff transform (WKT) and without Kirchhoff transform (NKT), in which the curves have a maximum difference ratio on the surface $x = 0$. Figure 6 shows the stress variations with Kirchhoff transform (WKT) and without Kirchhoff transform (NKT), in which the curves match at the surface according to the boundary condition of stress $(\sigma_{xx} = 0)$, then the difference ratio increases with the increase of distance until $x = 0.5$; after that the difference ratio decreases to reach zero at $x = 2.5$. Figures 7–9 display the variations of temperature, the variations of displacement, and the variations of stress along the distance x when $k_v = -0.5$. It was observed that there are highly different values between using the Kirchhoff transform (WKT) and not using Kirchhoff transform (NKT).

Figures 10–12 show the comparison between the numerical solution (finite element approach without Kirchhoff transform) and the analytical solution (Laplace transform and eigenvalues approach with Kirchhoff transform) when $K_v = 0$. The numerical results of temperature variation, displacement variations, and stress variations show good agreement with the findings of those analytical data over the distance x.

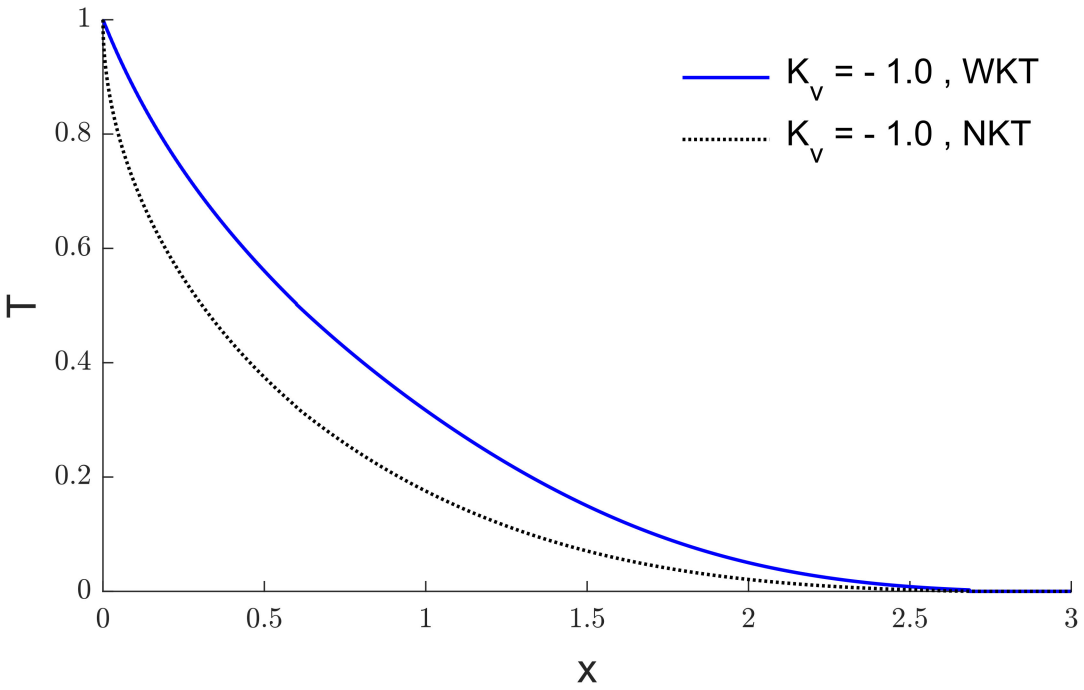

Figure 4. The temperature variation with and without Kirchhoff transform when $K_v = -1$.

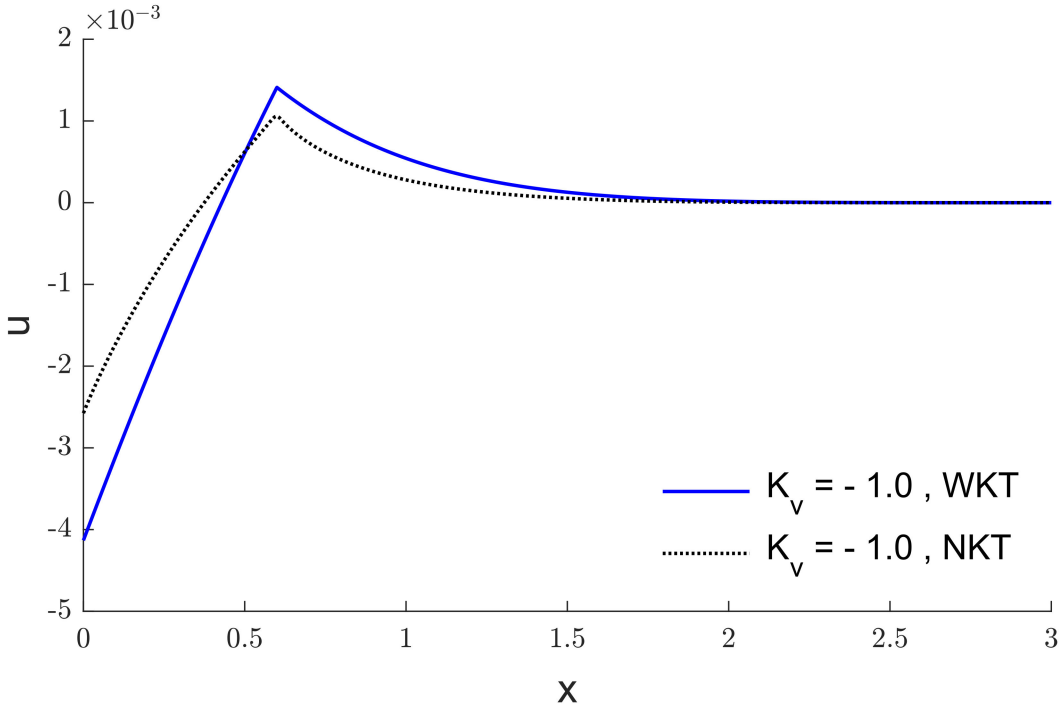

Figure 5. The displacement variation with and without Kirchhoff transform when $K_v = -1$.

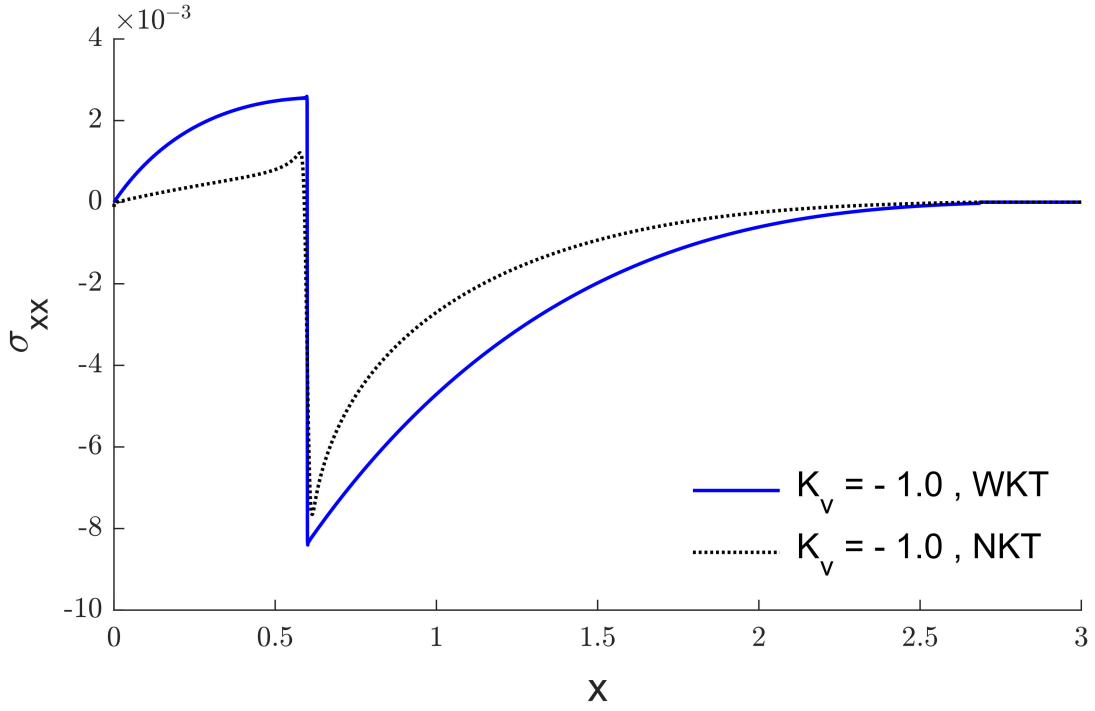

Figure 6. The stress variation with and without Kirchhoff transform when $K_v = -1$.

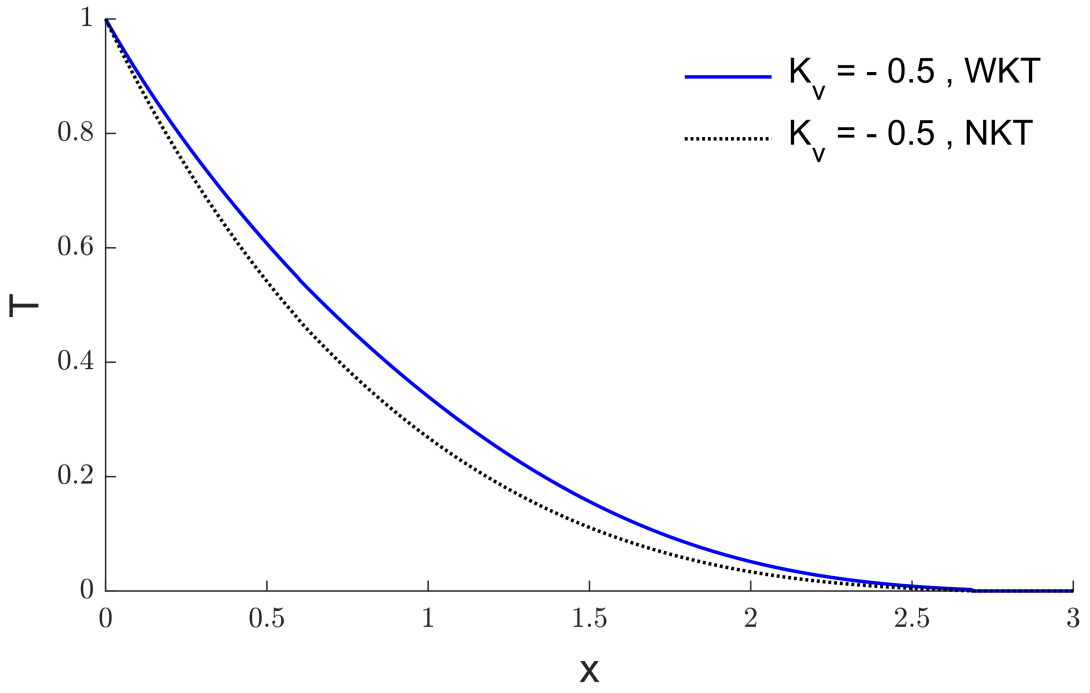

Figure 7. The temperature variations with and without Kirchhoff transform when $K_v = -0.5$.

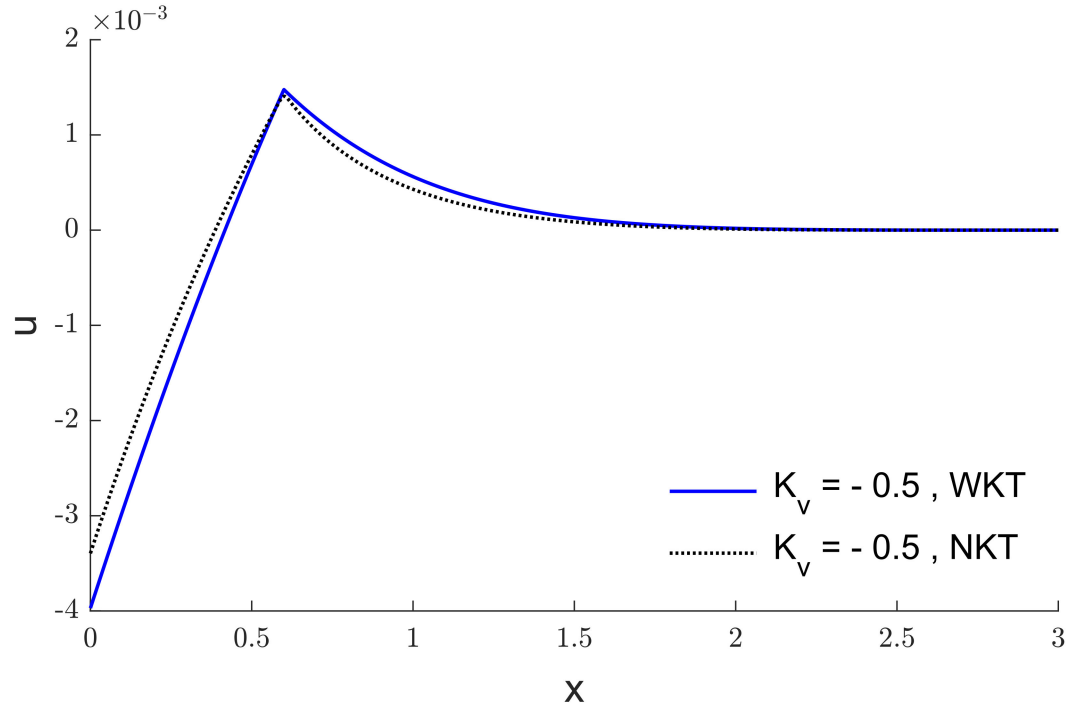

Figure 8. The displacement variation with and without Kirchhoff transform when $K_v = -0.5$.

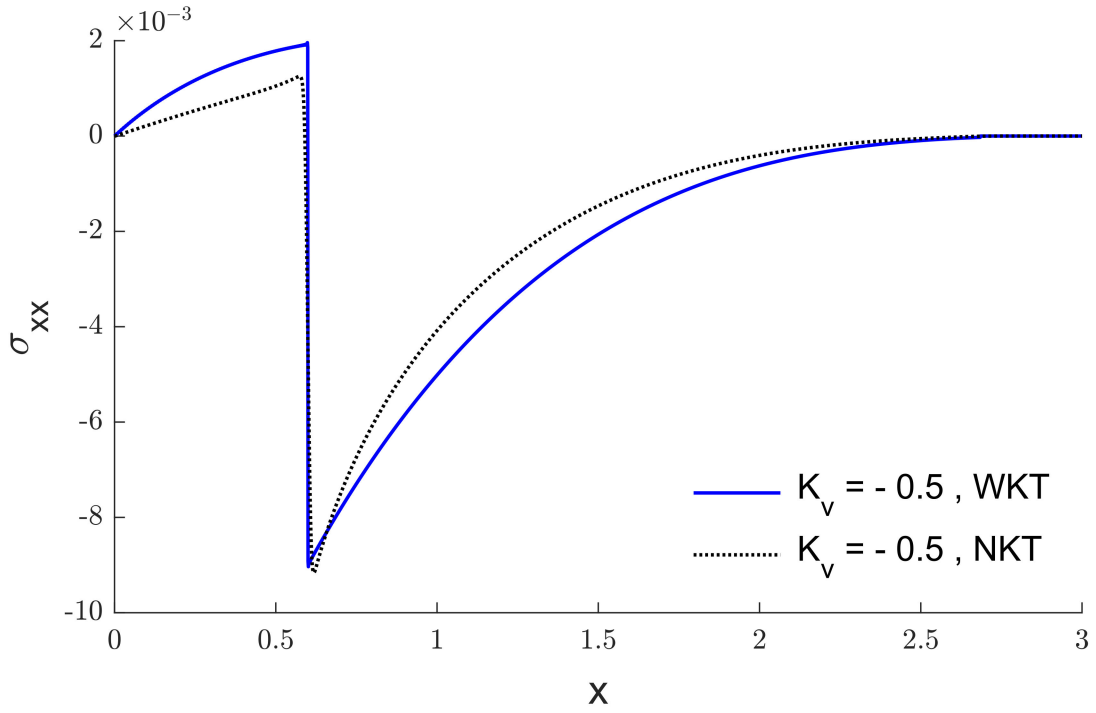

Figure 9. The stress variation with and without Kirchhoff transform when $K_v = -0.5$.

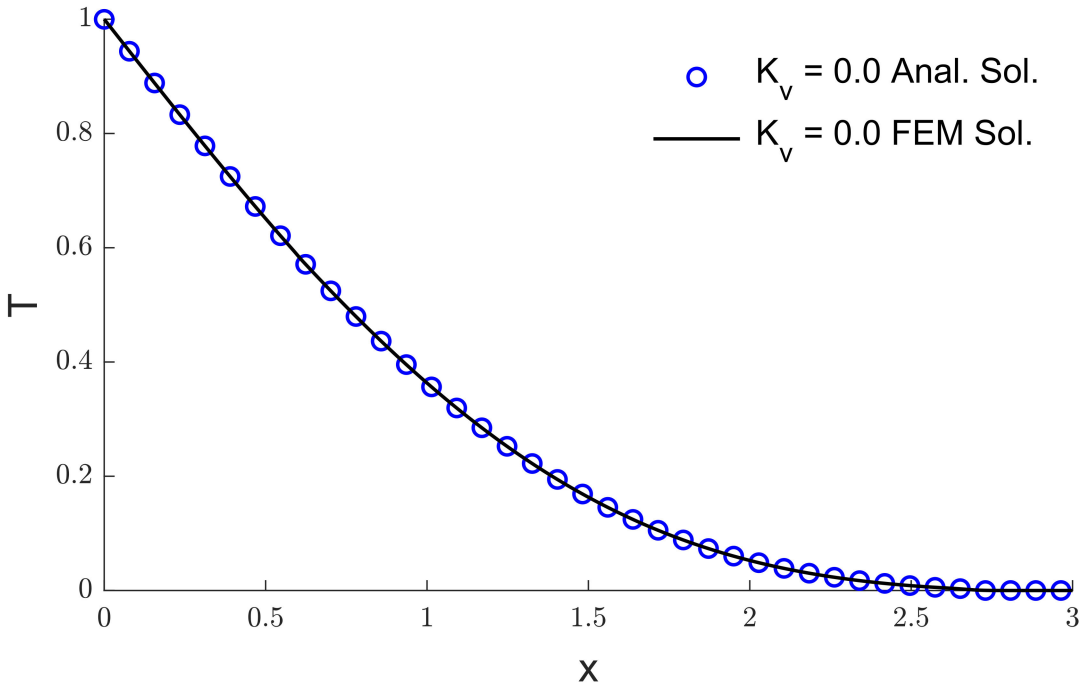

Figure 10. The temperature variation with and without Kirchhoff transform when $K_v = 0$.

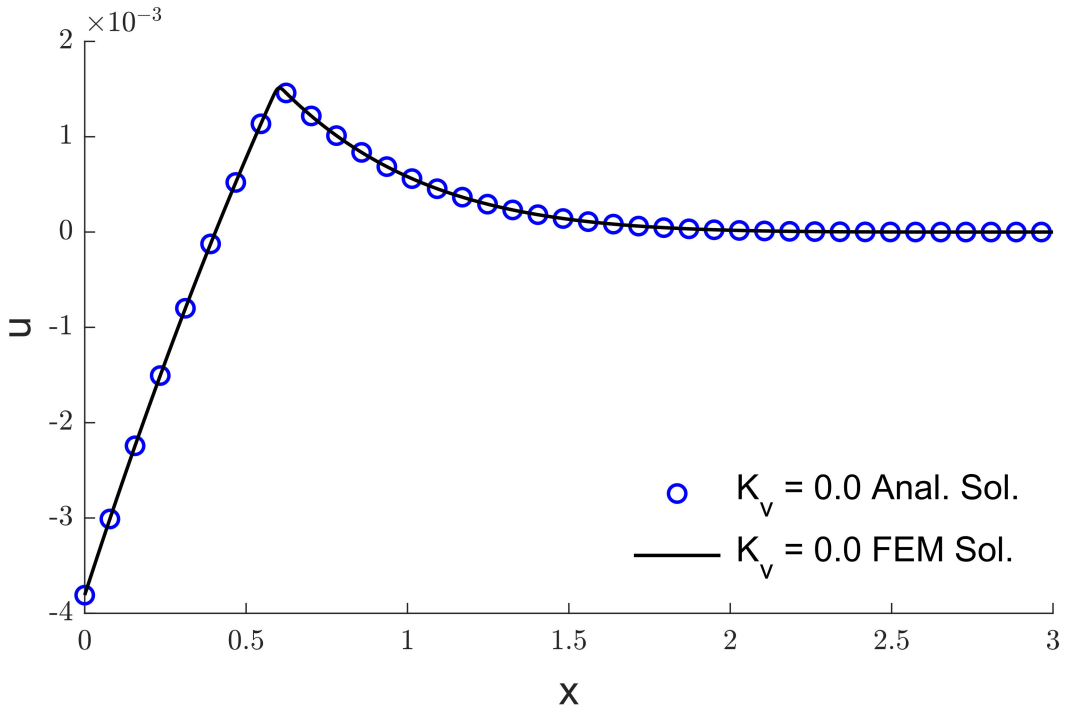

Figure 11. The displacement variation with and without Kirchhoff transform when $K_v = 0$.

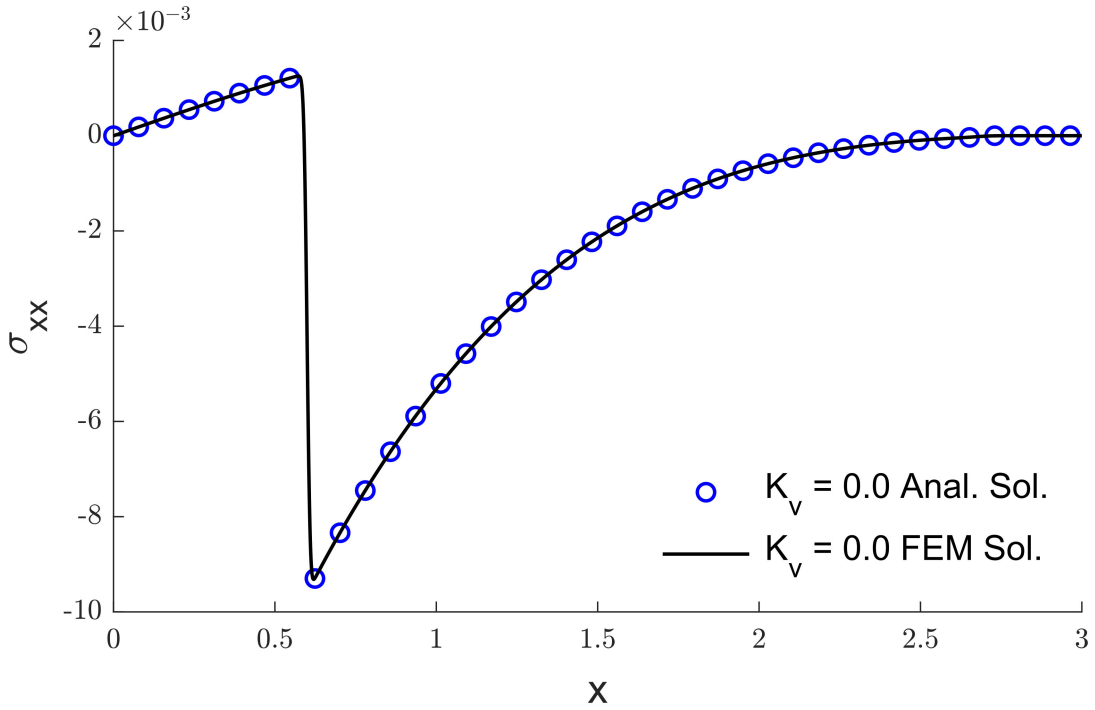

Figure 12. The stress variation with and without Kirchhoff transform when $K_v = 0$.

7. Conclusions

In this work, the effects of variable thermal conductivity with and without Kirchhoff's transformations in a thermoelastic medium are mathematically analyzed. The finite element method obtains the numerical solution for nonlinear equations without Kirchhoff's transformations. The eigenvalues method is used to obtain the analytical solution for nonlinear equations with Kirchhoff's transformations. It can thus be seen that the varying thermal conductivity has a significant impact and plays a role in the behaviors of deformations of different physical field components. Additionally, a comparison is made between the numerical and earlier analytical solutions produced by others while ignoring the new parameter, and the behavior of the solution is investigated to validate the proposed method's correctness.

Author Contributions: Conceptualization: A.H. and I.A.; methodology: A.H. and I.A.; validation: A.H. and I.A.; formal analysis: A.H. and I.A.; investigation: A.H. and I.A.; resources: I.A.; data curation: A.H. and I.A.; writing—original draft preparation: A.H. and I.A.; writing—review and editing: A.H.; visualization: I.A.; supervision: A.H. and I.A.; project administration: I.A. All authors have read and agreed to the published version of the manuscript.

Funding: This research work was funded by Institutional Fund Projects under grant no. (IFPIP: 8-130-1443). The authors gratefully acknowledge technical and financial support provided by the Ministry of Education and King Abdulaziz University, DSR, Jeddah, Saudi Arabia.

Institutional Review Board Statement: Not applicable.

Informed Consent Statement: Not applicable.

Data Availability Statement: Not applicable.

Conflicts of Interest: The authors declare no conflict of interest.

References

1. Noda, N. Thermal stresses in materials with temperature-dependent properties. *Appl. Mech. Rev.* **1991**, *44*, 383–397.
2. Lord, H.W.; Shulman, Y. A generalized dynamical theory of thermoelasticity. *J. Mech. Phys. Solids* **1967**, *15*, 299–309. [CrossRef]

3. Youssef, H.M.; Abbas, I.A. Thermal shock problem of generalized thermoelasticity for an infinitely long annular cylinder with variable thermal conductivity. *Comput. Methods Sci. Technol.* **2007**, *13*, 95–100.
4. Sherief, H.H.; Hamza, F.A. Modeling of variable thermal conductivity in a generalized thermoelastic infinitely long hollow cylinder. *Meccanica* **2016**, *51*, 551–558. [CrossRef]
5. Othman, M.I. Lord-Shulman theory under the dependence of the modulus of elasticity on the reference temperature in two-dimensional generalized thermoelasticity. *J. Therm. Stress.* **2002**, *25*, 1027–1045. [CrossRef]
6. Zenkour, A.M.; Abbas, I.A. A generalized thermoelasticity problem of an annular cylinder with temperature-dependent density and material properties. *Int. J. Mech. Sci.* **2014**, *84*, 54–60. [CrossRef]
7. Abbas, I.A. Generalized magneto-thermoelasticity in a nonhomogeneous isotropic hollow cylinder using the finite element method. *Arch. Appl. Mech.* **2009**, *79*, 41–50. [CrossRef]
8. Aboueregal, A.E.; Sedighi, H.M. The effect of variable properties and rotation in a visco-thermoelastic orthotropic annular cylinder under the Moore–Gibson–Thompson heat conduction model. *Proc. Inst. Mech. Eng. Part L J. Mat. Des. Appl.* **2021**, *235*, 1004–1020. [CrossRef]
9. Xiong, C.; Guo, Y. Effect of Variable Properties and Moving Heat Source on Magnetothermoelastic Problem under Fractional Order Thermoelasticity. *Adv. Mater. Sci. Eng.* **2016**, *2016*, 5341569. [CrossRef]
10. Singh, S.; Kumar, D.; Rai, K. Convective-radiative fin with temperature dependent thermal conductivity, heat transfer coefficient and wavelength dependent surface emissivity. *Propuls. Power Res.* **2014**, *3*, 207–221. [CrossRef]
11. Zhang, H.; Shang, C.; Tang, G. Measurement and identification of temperature-dependent thermal conductivity for thermal insulation materials under large temperature difference. *Int. J. Therm. Sci.* **2022**, *171*, 107261. [CrossRef]
12. Pan, W.; Yi, F.; Zhu, Y.; Meng, S. Identification of temperature-dependent thermal conductivity and experimental verification. *Meas. Sci. Technol.* **2016**, *27*, 075005. [CrossRef]
13. Wang, Y.Z.; Zan, C.; Liu, D.; Zhou, J.Z. Generalized solution of the thermoelastic problem for the axisymmetric structure with temperature-dependent properties. *Eur. J. Mech. A/Solids* **2019**, *76*, 346–354. [CrossRef]
14. Liang, W.; Huang, S.; Tan, W.S.; Wang, Y.Z. Asymptotic approach to transient thermal shock problem with variable material properties. *Mech. Adv. Mater. Struct.* **2019**, *26*, 350–358. [CrossRef]
15. Wang, Y.Z.; Liu, D.; Wang, Q.; Zhou, J.Z. Thermoelastic interaction in functionally graded thick hollow cylinder with temperature-dependent properties. *J. Therm. Stress.* **2018**, *41*, 399–417. [CrossRef]
16. Wang, Y.; Liu, D.; Wang, Q.; Zhou, J. Asymptotic solutions for generalized thermoelasticity with variable thermal material properties. *Arch. Mech.* **2016**, *68*, 181–202.
17. Wang, Y.; Liu, D.; Wang, Q.; Zhou, J. Problem of axisymmetric plane strain of generalized thermoelastic materials with variable thermal properties. *Eur. J. Mech. A/Solids* **2016**, *60*, 28–38. [CrossRef]
18. Wang, Y.; Liu, D.; Wang, Q.; Zhou, J. Effect of fractional order parameter on thermoelastic behaviors of elastic medium with variable properties. *Acta Mech. Solida Sin.* **2015**, *28*, 682–692. [CrossRef]
19. Ezzat, M.A.; El-Bary, A.A. On thermo-viscoelastic infinitely long hollow cylinder with variable thermal conductivity. *Microsyst. Technol.* **2017**, *23*, 3263–3270. [CrossRef]
20. Othman, M.I.A.; Abouelregal, A.E.; Said, S.M. The effect of variable thermal conductivity on an infinite fiber-reinforced thick plate under initial stress. *J. Mech. Mater. Struct.* **2019**, *14*, 277–293. [CrossRef]
21. Xiong, C.B.; Yu, L.N.; Niu, Y.B. Effect of Variable Thermal Conductivity on the Generalized Thermoelasticity Problems in a Fiber-Reinforced Anisotropic Half-Space. *Adv. Mater. Sci. Eng.* **2019**, *2019*, 8625371. [CrossRef]
22. Abbas, I.; Hobiny, A.; Marin, M. Photo-thermal interactions in a semi-conductor material with cylindrical cavities and variable thermal conductivity. *J. Taibah Univ. Sci.* **2020**, *14*, 1369–1376. [CrossRef]
23. Alzahrani, F. The Effects of Variable Thermal Conductivity in Semiconductor Materials Photogenerated by a Focused Thermal Shock. *Mathematics* **2020**, *8*, 1230.
24. Ghasemi, S.E.; Hatami, M.; Ganji, D.D. Thermal analysis of convective fin with temperature-dependent thermal conductivity and heat generation. *Case Stud. Therm. Eng.* **2014**, *4*, 1–8. [CrossRef]
25. Khoukhi, M.; Abdelbaqi, S.; Hassan, A. Transient temperature change within a wall embedded insulation with variable thermal conductivity. *Case Stud. Therm. Eng.* **2020**, *20*, 100645. [CrossRef]
26. Othman, M.I.A.; Tantawi, R.S.; Eraki, E.E.M. Effect of initial stress on a semiconductor material with temperature dependent properties under DPL model. *Microsyst. Technol.* **2017**, *23*, 5587–5598. [CrossRef]
27. Hobiny, A.; Alzahrani, F.; Abbas, I.; Marin, M. The effect of fractional time derivative of bioheat model in skin tissue induced to laser irradiation. *Symmetry* **2020**, *12*, 602. [CrossRef]
28. Abbas, I.A. A GN model for thermoelastic interaction in an unbounded fiber-reinforced anisotropic medium with a circular hole. *Appl. Math. Lett.* **2013**, *26*, 232–239. [CrossRef]
29. Li, C.; Guo, H.; Tian, X.; Tian, X. Transient response for a half-space with variable thermal conductivity and diffusivity under thermal and chemical shock. *J. Therm. Stress.* **2017**, *40*, 389–401. [CrossRef]
30. Marin, M.; Florea, O. On temporal behaviour of solutions in thermoelasticity of porous micropolar bodies. *An. Stiint. Univ. Ovidius Constanta Ser. Mat.* **2014**, *22*, 169–188. [CrossRef]
31. Bhatti, M.M.; Marin, M.; Zeeshan, A.; Abdelsalam, S.I. Editorial: Recent Trends in Computational Fluid Dynamics. *Front. Phys.* **2020**, *8*, 593111. [CrossRef]

32. Abouelregal, A.E.; Marin, M. The Size-Dependent Thermoelastic Vibrations of Nanobeams Subjected to Harmonic Excitation and Rectified Sine Wave Heating. *Mathematics* **2020**, *8*, 1128. [CrossRef]
33. Moradnouri, A.; Vakilian, M.; Hekmati, A.; Fardmanesh, M. Multi-segment Winding Application for Axial Short Circuit Force Reduction Under Tap Changer Operation in HTS Transformers. *J. Supercond. Nov. Magn.* **2019**, *32*, 3171–3182. [CrossRef]
34. Youssef, H. State-space approach on generalized thermoelasticity for an infinite material with a spherical cavity and variable thermal conductivity subjected to ramp-type heating. *Can. Appl. Math. Quaterly* **2005**, *13*, 369–390.
35. Abbas, I.A.; Kumar, R. Deformation due to thermal source in micropolar generalized thermoelastic half-space by finite element method. *J. Comput. Theor. Nanosci.* **2014**, *11*, 185–190.
36. Abbas, I.A. Eigenvalue approach on fractional order theory of thermoelastic diffusion problem for an infinite elastic medium with a spherical cavity. *Appl. Math. Model.* **2015**, *39*, 6196–6206. [CrossRef]
37. Othman, M.I.A.; Abbas, I.A. Eigenvalue approach for generalized thermoelastic porous medium under the effect of thermal loading due to a laser pulse in DPL model. *Indian J. Phys.* **2019**, *93*, 1567–1578. [CrossRef]
38. Kumar, R.; Miglani, A.; Rani, R. Eigenvalue formulation to micropolar porous thermoelastic circular plate using dual phase lag model. *Multidiscip. Model. Mater. Struct.* **2017**, *13*, 347–362. [CrossRef]
39. Kumar, R.; Miglani, A.; Rani, R. Analysis of micropolar porous thermoelastic circular plate by eigenvalue approach. *Arch. Mech.* **2016**, *68*, 423–439.
40. Gupta, N.D.; Das, N.C. Eigenvalue approach to fractional order generalized thermoelasticity with line heat source in an infinite medium. *J. Therm. Stress.* **2016**, *39*, 977–990. [CrossRef]
41. Santra, S.; Lahiri, A.; Das, N.C. Eigenvalue Approach on Thermoelastic Interactions in an Infinite Elastic Solid with Voids. *J. Therm. Stress.* **2014**, *37*, 440–454. [CrossRef]
42. Baksi, A.; Roy, B.K.; Bera, R.K. Eigenvalue approach to study the effect of rotation and relaxation time in generalized magneto-thermo-viscoelastic medium in one dimension. *Math. Comput. Model.* **2006**, *44*, 1069–1079. [CrossRef]
43. Das, N.C.; Lahiri, A.; Giri, R.R. Eigenvalue approach to generalized thermoelasticity. *Indian J. Pure Appl. Math.* **1997**, *28*, 1573–1594.
44. Stehfest, H. Algorithm 368: Numerical inversion of Laplace transforms [D5]. *Commun. ACM* **1970**, *13*, 47–49. [CrossRef]
45. Abbas, I.A.; Abdalla, A.E.N.N.; Alzahrani, F.S.; Spagnuolo, M. Wave propagation in a generalized thermoelastic plate using eigenvalue approach. *J. Therm. Stresses* **2016**, *39*, 1367–1377. [CrossRef]